PHYSICAL REVIEW D **92,** 114506 (2015)

Parity-expanded variational analysis for nonzero momentum

Finn M. Stokes,[1,*] Waseem Kamleh,[1] Derek B. Leinweber,[1] M. Selim Mahbub,[1,2]
Benjamin J. Menadue,[1,3] and Benjamin J. Owen[1]

[1]*Special Research Centre for the Subatomic Structure of Matter, Department of Physics, University of Adelaide, Adelaide, South Australia 5005, Australia*
[2]*Digital Productivity Flagship, CSIRO, 15 College Road, Sandy Bay, Tasmania 7005, Australia*
[3]*National Computational Infrastructure (NCI), Australian National University, Canberra, Australian Capital Territory 0200, Australia*

(Received 16 September 2015; published 15 December 2015)

In recent years, the use of variational analysis techniques in lattice QCD has been demonstrated to be successful in the investigation of the rest-mass spectrum of many hadrons. However, due to parity mixing, more care must be taken for investigations of boosted states to ensure that the projected correlation functions provided by the variational analysis correspond to the same states at zero momentum. In this paper we present the parity-expanded variational analysis (PEVA) technique, a novel method for ensuring the successful and consistent isolation of boosted baryons through a parity expansion of the operator basis used to construct the correlation matrix.

DOI: 10.1103/PhysRevD.92.114506 PACS numbers: 12.38.Gc, 12.38.Aw, 14.20.Gk

I. INTRODUCTION

One of the most widely recognized successes of lattice QCD has been its application to hadron spectroscopy [1–4]. The rest masses of not only the ground states but also many excited states can be extracted through a combination of effective mass techniques and variational analysis. Within the baryon sector alone significant progress has been made [5–12]. However, the study of excited states in lattice QCD is still a challenging endeavor and has not reached the maturity of ground state computations. This is particularly true in simulations near the physical value of the pion mass.

Once an understanding of the spectra is obtained, the logical progression is to investigate the structure of these hadrons, and again lattice QCD provides the tools needed for the precise determination of hadronic matrix elements. Key to lattice QCD's ability to investigate hadronic structure is the computation of two- and three-point correlation functions for each hadronic state of interest at both zero and nonzero final state momenta. While the zero momentum two-point case corresponds to the rest-mass analysis and is well understood, at nonzero momentum more care must be taken to ensure the energy eigenstates are cleanly extracted, especially when investigating excited states.

In this paper, we investigate the use of variational analysis techniques to extract correlation functions for excited states of spin-1/2 baryons at nonzero momentum. In Sec. II, we briefly describe the conventional approach and highlight how states of the opposite parity can intrude into the analysis. Section III demonstrates the parity-expanded variational analysis (PEVA) technique, a novel approach to overcoming this shortfall. This method will be central to future baryon form-factor calculations involving excited states, for example electromagnetic structure and transition analyses.

In Sec. IV, we present results comparing the conventional parity projection approach to the PEVA technique, demonstrating the removal of opposite-parity contaminations from two-point correlators through strong cross-parity contributions to the operator structure of the four lowest lying states. These results are calculated on the PACS-CS $(2+1)$-flavor full-QCD ensembles [1], made available through the ILDG [13]. They are $32^3 \times 64$ lattices with $\beta = 1.90$, and employ an Iwasaki gauge action with nonperturbatively $O(a)$-improved Wilson quarks. In particular, we demonstrate proof of principle on the ensemble with the second lightest quark mass. This ensemble consists of 400 gauge field configurations with $\kappa_{u,d} = 0.13770$, corresponding to a pion mass of 280 MeV.

II. PARITY MIXING AT NONZERO MOMENTUM

Eigenstates of nonzero momentum are not eigenstates of parity, so we categorize states by the way they transform in their rest frame. We call states that transform positively under parity in their rest frame "positive parity states" (and label them B^+), and states that transform negatively under parity in their rest frame "negative parity states" (B^-).

Conventional spin-1/2 baryon spectroscopy uses one or more operators $\{\chi^i\}$ which couple to both positive and negative parity states as

$$\langle \Omega | \chi^i | B^+; p; s \rangle = \lambda_i^{B^+} \sqrt{\frac{m_{B^+}}{E_{B^+}}} u_{B^+}(p,s), \tag{1a}$$

$$\langle \Omega | \chi^i | B^-; p; s \rangle = \lambda_i^{B^-} \sqrt{\frac{m_{B^-}}{E_{B^-}}} \gamma_5 u_{B^-}(p,s), \tag{1b}$$

*Corresponding author.
finn.stokes@adelaide.edu.au

and transform under parity as

$$\chi^i \to \gamma_4 \chi^i. \tag{2}$$

These operators are used to construct two-point correlation functions,

$$\mathcal{G}_{ij}(\boldsymbol{p}, t) \equiv \sum_{\boldsymbol{x}} \mathrm{e}^{-\mathrm{i}\boldsymbol{p}\cdot\boldsymbol{x}} \langle \Omega | \chi^i(x) \bar{\chi}^j(0) | \Omega \rangle, \tag{3}$$

which in the Pauli representation have the Dirac structure

$$\mathcal{G}_{ij}(\boldsymbol{p}, t) = \sum_{B^\pm} \mathrm{e}^{-E_{B^\pm} t} \lambda_i^{B^\pm} \bar{\lambda}_j^{B^\pm} \frac{-\mathrm{i}\gamma \cdot p \pm m_{B^\pm}}{2E_{B^\pm}} \tag{4}$$

(for more details see Sec. III).

For clarity, Eq. (4) is formulated for the case of a fixed boundary condition in the temporal direction, as used herein. It is also applicable to the common case of an (anti-)periodic boundary condition in the temporal direction on lattices with large Euclidean time extents where the contributions of backward-running baryon states are negligible. The case of non-negligible backward-running states is presented at the end of Sec. III A.

These correlation functions contain states of both parities, so conventionally we take the spinor trace with some projector Γ, defining $G_{ij}(\Gamma; \boldsymbol{p}, t) \equiv \mathrm{tr}(\Gamma \mathcal{G}_{ij}(\boldsymbol{p}, t))$. If we choose $\Gamma = \Gamma^\pm \equiv (\gamma_4 \pm \mathrm{I})/2$, we get the parity-projected correlators

$$\begin{aligned} G_{ij}(\Gamma^\pm; \boldsymbol{p}, t) &\equiv \mathrm{tr}(\Gamma^\pm \mathcal{G}_{ij}(\boldsymbol{p}, t)) \\ &= \sum_{B^+} \mathrm{e}^{-E_{B^+} t} \lambda_i^{B^+} \bar{\lambda}_j^{B^+} \frac{E_{B^+} \pm m_{B^+}}{2E_{B^+}} \\ &\quad + \sum_{B^-} \mathrm{e}^{-E_{B^-} t} \lambda_i^{B^-} \bar{\lambda}_j^{B^-} \frac{E_{B^-} \mp m_{B^-}}{2E_{B^-}}. \end{aligned} \tag{5}$$

At zero momentum, $E_B = m_B$, so the parity-projected correlators contain only positive or negative parity states:

$$G_{ij}(\Gamma^+; \boldsymbol{0}; t) = \sum_{B^+} \mathrm{e}^{-m_{B^+} t} \lambda_i^{B^+} \bar{\lambda}_j^{B^+}, \tag{6a}$$

$$G_{ij}(\Gamma^-; \boldsymbol{0}; t) = \sum_{B^-} \mathrm{e}^{-m_{B^-} t} \lambda_i^{B^-} \bar{\lambda}_j^{B^-}. \tag{6b}$$

However, at nonzero momentum, $E_B \neq m_B$ and the parity-projected correlators include $O((E-m)/2E)$ opposite-parity contaminations. This situation was investigated in [14], where a projector of the form

$$\Gamma^\pm(\boldsymbol{p}) \equiv \frac{1}{2}\left(\frac{m_{B_0^\mp}}{E_{B_0^\mp}(\boldsymbol{p})} \gamma_0 \pm \mathrm{I} \right) \tag{7}$$

was introduced to remove a single contaminating state, the lowest state of the opposite parity. However, if there is more than one nearby state contaminating the correlation function, the additional contaminating state will still remain.

Another option is to take the trace with γ_4 to get

$$G_{ij}(\gamma_4; \boldsymbol{p}, t) = \sum_{B} \mathrm{e}^{-E_B t} \lambda_i^B \bar{\lambda}_j^B, \tag{8}$$

where the sum over B now contains both parities. We can then use standard correlation matrix techniques to isolate the excited state spectrum of both parities simultaneously. However, we are isolating both positive and negative parity states in a single correlation matrix rather than in separate positive and negative parity-projected correlation matrices. For a given operator basis, we are hence only able to isolate half as many states of each parity. We are also destroying the parity information encoded in the Dirac structure, preventing one from distinguishing whether a particular state has positive or negative rest-frame parity. A technique similar to this appears to be used by Lang and Verduci in [10].

III. USING AN EXPANDED OPERATOR BASIS

A. Physics at the hadronic level

We wish to expand the operator basis of the correlation matrix with operators that utilize the Dirac structure to isolate energy eigenstates while maintaining a signature of their rest-frame parity. By considering the Dirac structure of the correlation function $\sum_{\boldsymbol{x}} \mathrm{e}^{-\mathrm{i}\boldsymbol{p}\cdot\boldsymbol{x}} \langle \Omega | \gamma_5 \chi^i(x) \bar{\chi}^j(0) | \Omega \rangle$ (which captures the cross-parity mixing), we find that the on-diagonal blocks are proportional to $\sigma_k p_k$. To access this signal, we need a projector with a $\gamma_5 \gamma_k \hat{p}_k$ term. Hence, we introduce a novel momentum-dependent projector $\Gamma_{\boldsymbol{p}} \equiv \frac{1}{4}(\mathrm{I} + \gamma_4)(\mathrm{I} - \mathrm{i}\gamma_5 \gamma_k \hat{p}_k)$ which allows us to construct a set of "parity-signature" projected operators

$$\chi_{\boldsymbol{p}}^i = \Gamma_{\boldsymbol{p}} \chi^i, \tag{9a}$$

$$\chi_{\boldsymbol{p}}^{i'} = \Gamma_{\boldsymbol{p}} \gamma_5 \chi^i. \tag{9b}$$

The primed indices denote the inclusion of γ_5, inverting the way the operators transform under parity.

Unlike the conventional baryon interpolators χ^i, these operators have definite parity at zero momentum and hence transform as eigenstates of parity

$$\chi_{\boldsymbol{0}}^i \to \chi_{\boldsymbol{0}}^i, \tag{10a}$$

$$\chi_{\boldsymbol{0}}^{i'} \to -\chi_{\boldsymbol{0}}^{i'}. \tag{10b}$$

Making use of this property at zero momentum, we introduce the nomenclature that operators with unprimed indices are "positive parity operators" (χ^+) and operators with primed indices are "negative parity operators" (χ^-). We use these terms in quotes here as these operators are only definite in parity at zero momentum, and while the

operators at nonzero momentum have a clear connection to the definite parity operators at zero momentum, they are not themselves definite in parity.

Drawing on the spinor structure for an on-shell baryon of momentum $\boldsymbol{p}$, we find that

$$\Gamma_{\boldsymbol{p}} u(p,\uparrow) = \frac{1}{4}(\mathrm{I}+\gamma_4)(\mathrm{I}-\mathrm{i}\gamma_5\gamma_k\hat{p}_k)\begin{pmatrix} 1 \\ 0 \\ \frac{p_3}{E+m} \\ \frac{p_1+\mathrm{i}p_2}{E+m} \end{pmatrix} = \frac{1}{2}\begin{pmatrix} 1-\hat{p}_3 \\ -\hat{p}_1-\mathrm{i}\hat{p}_2 \\ 0 \\ 0 \end{pmatrix}, \tag{11a}$$

and

$$\Gamma_{\boldsymbol{p}}\gamma_5 u(p,\uparrow) = \frac{1}{4}(\mathrm{I}+\gamma_4)(\mathrm{I}-\mathrm{i}\gamma_5\gamma_k\hat{p}_k)\begin{pmatrix} \frac{-p_3}{E+m} \\ \frac{-p_1-\mathrm{i}p_2}{E+m} \\ -1 \\ 0 \end{pmatrix} = \frac{1}{2}\frac{|\boldsymbol{p}|}{E+m}\begin{pmatrix} 1-\hat{p}_3 \\ -\hat{p}_1-\mathrm{i}\hat{p}_2 \\ 0 \\ 0 \end{pmatrix}. \tag{11b}$$

Thus, $\Gamma_{\boldsymbol{p}}\gamma_5 u(p,\uparrow) = \frac{|\boldsymbol{p}|}{E+m}\Gamma_{\boldsymbol{p}} u(p,\uparrow)$. Similarly, we find that $\Gamma_{\boldsymbol{p}}\gamma_5 u(p,\downarrow) = \frac{|\boldsymbol{p}|}{E+m}\Gamma_{\boldsymbol{p}} u(p,\downarrow)$. Thus, these operators couple to the states of interest with a consistent Dirac structure,

$$\langle\Omega|\chi^i_{\boldsymbol{p}}|B^+;p;s\rangle = \lambda_i^{B^+}\sqrt{\frac{m_{B^+}}{E_{B^+}}}\Gamma_{\boldsymbol{p}} u_{B^+}(p,s), \tag{12a}$$

$$\langle\Omega|\chi^i_{\boldsymbol{p}}|B^-;p;s\rangle = \lambda_i^{B^-}\frac{|\boldsymbol{p}|}{E_{B^-}+m_{B^-}}\sqrt{\frac{m_{B^-}}{E_{B^-}}}\Gamma_{\boldsymbol{p}} u_{B^-}(p,s), \tag{12b}$$

$$\langle\Omega|\chi^{i'}_{\boldsymbol{p}}|B^+;p;s\rangle = \lambda_i^{B^+}\frac{|\boldsymbol{p}|}{E_{B^+}+m_{B^+}}\sqrt{\frac{m_{B^+}}{E_{B^+}}}\Gamma_{\boldsymbol{p}} u_{B^+}(p,s), \tag{12c}$$

$$\langle\Omega|\chi^{i'}_{\boldsymbol{p}}|B^-;p;s\rangle = \lambda_i^{B^-}\sqrt{\frac{m_{B^-}}{E_{B^-}}}\Gamma_{\boldsymbol{p}} u_{B^-}(p,s). \tag{12d}$$

At zero momentum, $\chi^i_{\boldsymbol{p}}$ and $\chi^{i'}_{\boldsymbol{p}}$ couple only to states of positive and negative parity respectively. However, as we boost to nonzero momenta, the operators couple to states of both parities.

We seek a set of "perfect" operators $\{\phi^\alpha_{\boldsymbol{p}}\}$ that perfectly isolate energy eigenstates, that is,

$$\langle\Omega|\phi^\alpha_{\boldsymbol{p}}|B^\beta;p;s\rangle = \delta^{\alpha\beta}\sqrt{\frac{m_\alpha}{E_\alpha}}z^\alpha\Gamma_{\boldsymbol{p}} u_\alpha(p,s). \tag{13}$$

Using the linearity of the operator space, and assuming that the set $\{\chi^i_{\boldsymbol{p}},\chi^{i'}_{\boldsymbol{p}}\}$ spans the whole space, the perfect operators can be written as linear combinations of these operators:

$$\phi^\alpha_{\boldsymbol{p}} = \sum_i v_i^\alpha(\boldsymbol{p})\chi^i_{\boldsymbol{p}} + \sum_{i'} v_{i'}^\alpha(\boldsymbol{p})\chi^{i'}_{\boldsymbol{p}}, \tag{14a}$$

$$\bar{\phi}^\alpha_{\boldsymbol{p}} = \sum_i u_i^\alpha(\boldsymbol{p})\bar{\chi}^i_{\boldsymbol{p}} + \sum_{i'} u_{i'}^\alpha(\boldsymbol{p})\bar{\chi}^{i'}_{\boldsymbol{p}}. \tag{14b}$$

To find the values of the coefficients $v_i^\alpha(\boldsymbol{p})$, $v_{i'}^\alpha(\boldsymbol{p})$, $u_i^\alpha(\boldsymbol{p})$, and $u_{i'}^\alpha(\boldsymbol{p})$, we consider the correlation matrix $\mathcal{G}(\boldsymbol{p},t)$ formed from the blocks

$$\mathcal{G}_{ij}(\boldsymbol{p},t) \equiv \sum_{\boldsymbol{x}} \mathrm{e}^{-\mathrm{i}\boldsymbol{p}\cdot\boldsymbol{x}}\langle\Omega|\chi^i_{\boldsymbol{p}}(x)\bar{\chi}^j_{\boldsymbol{p}}(0)|\Omega\rangle, \tag{15a}$$

$$\mathcal{G}_{ij'}(\boldsymbol{p},t) \equiv \sum_{\boldsymbol{x}} \mathrm{e}^{-\mathrm{i}\boldsymbol{p}\cdot\boldsymbol{x}}\langle\Omega|\chi^i_{\boldsymbol{p}}(x)\bar{\chi}^{j'}_{\boldsymbol{p}}(0)|\Omega\rangle, \tag{15b}$$

$$\mathcal{G}_{i'j}(\boldsymbol{p},t) \equiv \sum_{\boldsymbol{x}} \mathrm{e}^{-\mathrm{i}\boldsymbol{p}\cdot\boldsymbol{x}}\langle\Omega|\chi^{i'}_{\boldsymbol{p}}(x)\bar{\chi}^j_{\boldsymbol{p}}(0)|\Omega\rangle, \tag{15c}$$

$$\mathcal{G}_{i'j'}(\boldsymbol{p},t) \equiv \sum_{\boldsymbol{x}} \mathrm{e}^{-\mathrm{i}\boldsymbol{p}\cdot\boldsymbol{x}}\langle\Omega|\chi^{i'}_{\boldsymbol{p}}(x)\bar{\chi}^{j'}_{\boldsymbol{p}}(0)|\Omega\rangle. \tag{15d}$$

By inserting a complete set of states $\mathrm{I} = \sum_{B,s}|B;p;s\rangle\langle B;p;s|$ between the operators, and noting our use of Euclidean time and fixed boundary conditions (or negligible backward-running state contributions), we can rewrite the correlation matrix as

$$\mathcal{G}_{ij}(\boldsymbol{p},t) = \sum_{B,s}\mathrm{e}^{-E_B t}\langle\Omega|\chi^i_{\boldsymbol{p}}(0)|B;p;s\rangle\langle B;p;s|\bar{\chi}^j_{\boldsymbol{p}}(0)|\Omega\rangle, \tag{16}$$

et cetera.

By substituting in the expressions from Eq. (15), and using the relation $\Gamma_{\boldsymbol{p}}(-\mathrm{i}\gamma\cdot p + m_B)\Gamma_{\boldsymbol{p}} = \Gamma_{\boldsymbol{p}}(E_B + m_B)$, we can rearrange each block to factor out the Dirac structure [see Eq. (A1) in the Appendix], giving

$$\mathcal{G}_{ij}(\boldsymbol{p},t) = \Gamma_{\boldsymbol{p}}\left[\sum_{B^\pm}\mathrm{e}^{-E_{B^\pm}t}\lambda_i^{B^\pm}\bar{\lambda}_j^{B^\pm}\frac{E_{B^\pm}\pm m_{B^\pm}}{2E_{B^\pm}}\right], \tag{17a}$$

$$\mathcal{G}_{ij'}(\boldsymbol{p},t) = \Gamma_{\boldsymbol{p}}\left[\sum_{B^\pm}\mathrm{e}^{-E_{B^\pm}t}\lambda_i^{B^\pm}\bar{\lambda}_j^{B^\pm}\frac{|\boldsymbol{p}|}{2E_{B^\pm}}\right], \tag{17b}$$

$$\mathcal{G}_{i'j}(\boldsymbol{p},t) = \Gamma_p \left[\sum_{B^\pm} \mathrm{e}^{-E_{B^\pm} t} \lambda_i^{B^\pm} \bar{\lambda}_j^{B^\pm} \frac{|\boldsymbol{p}|}{2E_{B^\pm}} \right], \tag{17c}$$

$$\mathcal{G}_{i'j'}(\boldsymbol{p},t) = \Gamma_p \left[\sum_{B^\pm} \mathrm{e}^{-E_{B^\pm} t} \lambda_i^{B^\pm} \bar{\lambda}_j^{B^\pm} \frac{E_{B^\pm} \mp m_{B^\pm}}{2E_{B^\pm}} \right]. \tag{17d}$$

Noting that $\mathrm{tr}(\Gamma_p) = 1$, the spinor trace of the correlation matrix $\mathcal{G}(\boldsymbol{p},t)$, denoted $G(\boldsymbol{p},t)$, obeys the relation $\mathcal{G}(\boldsymbol{p},t) = \Gamma_p G(\boldsymbol{p},t)$.

Now, if we right multiply the traced correlation matrix $G(\boldsymbol{p},t)$ by the column vector

$$\boldsymbol{u}^{\alpha^+}(\boldsymbol{p}) \equiv (u_1^{\alpha^+}(\boldsymbol{p}), \ldots, u_n^{\alpha^+}(\boldsymbol{p}), u_{1'}^{\alpha^+}(\boldsymbol{p}), \ldots, u_{n'}^{\alpha^+}(\boldsymbol{p}))^\top$$

corresponding to the positive parity state B^{α^+}, then the components of the resulting vector are given by

$$(G(\boldsymbol{p},t)\boldsymbol{u}^{\alpha^+}(\boldsymbol{p}))_i = \mathrm{e}^{-E_{\alpha^+} t} \lambda_i^{\alpha^+} \bar{z}^{\alpha^+} \frac{E_{\alpha^+} + m_{\alpha^+}}{2E_{\alpha^+}}, \tag{18a}$$

$$(G(\boldsymbol{p},t)\boldsymbol{u}^{\alpha^+}(\boldsymbol{p}))_{i'} = \mathrm{e}^{-E_{\alpha^+} t} \lambda_i^{\alpha^+} \bar{z}^{\alpha^+} \frac{|\boldsymbol{p}|}{2E_{\alpha^+}}. \tag{18b}$$

Details are provided in Eq. (A2) of the Appendix.

Note that both the primed and unprimed components depend on the same coupling parameters $\lambda_i^{\alpha^+}$. So, putting together the components from Eqs. (18a) and (18b), the full vector is given by $G(\boldsymbol{p},t)\boldsymbol{u}^{\alpha^+}(\boldsymbol{p}) = \boldsymbol{\lambda}^{\alpha^+} \bar{z}^{\alpha^+} \mathrm{e}^{-E_{\alpha^+} t}$, for an appropriately defined vector $\boldsymbol{\lambda}^{\alpha^+}$.

Similarly, for $\boldsymbol{u}^{\alpha^-}(\boldsymbol{p})$ corresponding to the negative parity state B^{α^-}, $G(\boldsymbol{p},t)\boldsymbol{u}^{\alpha^-}(\boldsymbol{p}) = \mathrm{e}^{-E_{\alpha^-} t} \boldsymbol{\lambda}^{\alpha^-} \bar{z}^{\alpha^-}$.

Now if we instead consider left multiplication by the row vector

$$\boldsymbol{v}^\alpha(\boldsymbol{p}) \equiv (v_1^\alpha(\boldsymbol{p}), \ldots, v_n^\alpha(\boldsymbol{p}), v_{1'}^\alpha(\boldsymbol{p}), \ldots, v_{n'}^\alpha(\boldsymbol{p})),$$

we get

$$\boldsymbol{v}^\alpha(\boldsymbol{p}) G(\boldsymbol{p},t) = z^\alpha \bar{\boldsymbol{\lambda}}^\alpha \mathrm{e}^{-E_\alpha t}. \tag{19}$$

Moreover, if we sandwich $G(\boldsymbol{p},t)$ between $\boldsymbol{v}^\alpha(\boldsymbol{p})$ and $\boldsymbol{u}^\beta(\boldsymbol{p})$, we get

$$\boldsymbol{v}^\alpha(\boldsymbol{p}) G(\boldsymbol{p},t) \boldsymbol{u}^\beta(\boldsymbol{p}) = \mathrm{e}^{-E_\alpha t} z^\alpha \bar{z}^\beta \delta^{\alpha\beta} \frac{E_\alpha + m_\alpha}{2E_\alpha}. \tag{20}$$

Thus, we can construct correlation functions that contain single energy eigenstates by sandwiching $G(\boldsymbol{p},t)$ between $\boldsymbol{v}^\alpha(\boldsymbol{p})$ and $\boldsymbol{u}^\alpha(\boldsymbol{p})$, giving

$$\begin{aligned} G^\alpha(\boldsymbol{p},t) &\equiv \boldsymbol{v}^\alpha(\boldsymbol{p}) G(\boldsymbol{p},t) \boldsymbol{u}^\alpha(\boldsymbol{p}) \\ &= \mathrm{e}^{-E_\alpha t} z^\alpha \bar{z}^\alpha \frac{E_\alpha + m_\alpha}{2E_\alpha}. \end{aligned} \tag{21}$$

Since the t dependence of both $G(\boldsymbol{p},t)\boldsymbol{u}^\alpha(\boldsymbol{p})$ and $\boldsymbol{v}^\alpha(\boldsymbol{p})G(\boldsymbol{p},t)$ is constrained to the exponential, we can express it via the recurrence relations

$$G(\boldsymbol{p},t+\Delta t)\boldsymbol{u}^\alpha(\boldsymbol{p}) = \mathrm{e}^{-E_\alpha(\boldsymbol{p})\Delta t} G(\boldsymbol{p},t)\boldsymbol{u}^\alpha(\boldsymbol{p}), \tag{22a}$$

$$\boldsymbol{v}^\alpha(\boldsymbol{p}) G(\boldsymbol{p},t+\Delta t) = \mathrm{e}^{-E_\alpha(\boldsymbol{p})\Delta t} \boldsymbol{v}^\alpha(\boldsymbol{p}) G(\boldsymbol{p},t). \tag{22b}$$

That is, $\boldsymbol{u}^\alpha(\boldsymbol{p})$ and $\boldsymbol{v}^\alpha(\boldsymbol{p})$ are respectively the right and left generalized eigenvectors of $G(\boldsymbol{p},t+\Delta t)$ and $G(\boldsymbol{p},t)$, with generalized eigenvalue $\mathrm{e}^{-E_\alpha(\boldsymbol{p})\Delta t}$.

In the case of non-negligible backward-running states on an (anti-)periodic lattice with temporal extent T, we can generalize Eq. (16) to include the backward-running baryons as in the meson case [15]:

$$\begin{aligned} &\mathcal{G}_{ij}(\boldsymbol{p},t) \\ &\quad = \sum_{B,s} \mathrm{e}^{-E_B t} \quad \langle \Omega | \chi_{\boldsymbol{p}}^i(0) | B;p;s \rangle \langle B;p;s | \bar{\chi}_{\boldsymbol{p}}^j(0) | \Omega \rangle \\ &\qquad \mp \sum_{\bar{B},s} \mathrm{e}^{-E_B (T-t)} \quad \langle \Omega | \bar{\chi}_{\boldsymbol{p}}^j(0) | \bar{B};p;s \rangle \langle \bar{B};p;s | \chi_{\boldsymbol{p}}^i(0) | \Omega \rangle, \end{aligned} \tag{23}$$

where the outer product of Dirac spinor indices is implicit and the sign of the second term reflects periodic/antiperiodic boundary conditions respectively, with the source on the boundary.

The operator overlaps for the backward-running baryons are given by

$$\langle \bar{B}^+;p;s|\chi_{\boldsymbol{p}}^i|\Omega\rangle = \lambda_i^{B^-} \sqrt{\frac{m_{B^-}}{E_{B^-}}} \Gamma_p \gamma_5 v_{\bar{B}^+}(p,s), \tag{24a}$$

$$\langle \bar{B}^-;p;s|\chi_{\boldsymbol{p}}^i|\Omega\rangle = \lambda_i^{B^+} \frac{|\boldsymbol{p}|}{E_{B^-} + m_{B^-}} \sqrt{\frac{m_{B^+}}{E_{B^+}}} \Gamma_p \gamma_5 v_{\bar{B}^-}(p,s), \tag{24b}$$

$$\langle \bar{B}^+;p;s|\chi_{\boldsymbol{p}}^{i'}|\Omega\rangle = \lambda_i^{B^-} \frac{|\boldsymbol{p}|}{E_{B^-} + m_{B^-}} \sqrt{\frac{m_{B^-}}{E_{B^-}}} \Gamma_p \gamma_5 v_{\bar{B}^+}(p,s), \tag{24c}$$

$$\langle \bar{B}^-;p;s|\chi_{\boldsymbol{p}}^{i'}|\Omega\rangle = \lambda_i^{B^+} \sqrt{\frac{m_{B^+}}{E_{B^+}}} \Gamma_p \gamma_5 v_{\bar{B}^-}(p,s). \tag{24d}$$

With these definitions, the formalism described above may be applied in the same manner, noting that

$$\sum_s v_{\bar{B}^\pm}(p,s)\bar{v}_{\bar{B}^\pm}(p,s) = -\frac{i\gamma\cdot p + m_{B^\mp}}{2m_{B^\mp}}. \quad (25)$$

The backward-running states will appear as negative-energy opposite-parity partners to each of the forward-running states, with couplings suppressed by a factor of $e^{-E_B T}$. Thus, given a sufficiently large operator basis, the PEVA technique can be used unmodified to simultaneously isolate both forward-running states and their backward-running partners.

B. Calculation at the quark level

To simplify the numerical calculation of $G(\boldsymbol{p},t)$, we use the idempotence of $\Gamma_{\boldsymbol{p}}$ and the invariance of the trace operation under cyclic permutations to rewrite it as

$$\begin{aligned} G_{ij}(\boldsymbol{p},t) &= \mathrm{tr}\left(\sum_{\boldsymbol{x}} e^{-i\boldsymbol{p}\cdot\boldsymbol{x}}\langle\Omega|\Gamma_{\boldsymbol{p}}\chi^i(x)\bar{\chi}^j(0)\Gamma_{\boldsymbol{p}}|\Omega\rangle\right) \\ &= \mathrm{tr}\left(\Gamma_{\boldsymbol{p}}\sum_{\boldsymbol{x}} e^{-i\boldsymbol{p}\cdot\boldsymbol{x}}\langle\Omega|\chi^i(x)\bar{\chi}^j(0)|\Omega\rangle\right) \\ &= G_{ij}(\Gamma_{\boldsymbol{p}};\boldsymbol{p},t), \end{aligned} \quad (26)$$

and similarly

$$G_{ij'}(\boldsymbol{p},t) = G_{ij}(-\gamma_5\Gamma_{\boldsymbol{p}};\boldsymbol{p},t), \quad (27a)$$

$$G_{i'j}(\boldsymbol{p},t) = G_{ij}(\Gamma_{\boldsymbol{p}}\gamma_5;\boldsymbol{p},t), \quad (27b)$$

$$G_{i'j'}(\boldsymbol{p},t) = G_{ij}(-\gamma_5\Gamma_{\boldsymbol{p}}\gamma_5;\boldsymbol{p},t). \quad (27c)$$

Thus if we consider N interpolators, χ^i, $i = 1, \ldots, N$, we can calculate each of the four $N\times N$ blocks of our full $2N\times 2N$ correlation matrix simply by taking the spinor trace of the unprojected correlators with the appropriate combination of $\Gamma_{\boldsymbol{p}}$ and γ_5, much like we would with $\Gamma_\pm$ in a conventional parity projection at $\boldsymbol{p}=0$.

At zero momentum, the off-diagonal blocks $G_{ij'}(\boldsymbol{p},t)$ and $G_{i'j}(\boldsymbol{p},t)$ will be zero, as they are proportional to $|\boldsymbol{p}|$, so we can treat the top-left and bottom-right blocks separately. Since at zero momentum $\chi^i_{\boldsymbol{p}}$ couples only to positive parity states and $\chi^{i'}_{\boldsymbol{p}}$ couples only to negative parity states, the top-left block will contain only positive parity states and the bottom-right only negative. Thus, we can solve the generalized eigenvalue equation for the positive and negative parity sectors separately. This is equivalent to the conventional parity-projected analysis using $\Gamma^\pm = \frac{1}{2}(\gamma_4 \pm \mathrm{I})$. However, at nonzero momentum there will be contributions from states of both parities in all four blocks, and the conventional technique will suffer from opposite-parity contaminations. The PEVA technique addresses this problem by utilizing a parity-expanded basis to simultaneously isolate energy eigenstates of both rest-frame parities.

IV. RESULTS

As a first investigation of the PEVA approach, we isolate the four lowest lying states of the nucleon on the lattice (the ground state, the first two negative parity excitations, and the first positive parity excitation). We consider the conventional parity projectors Γ^+ and Γ^- acting on an 8×8 correlation matrix as well as the PEVA technique, which expands this to a 16×16 correlation matrix. The original eight-operator basis is formed from the conventional spin-1/2 nucleon operators $\chi_1 = \epsilon^{abc}[u^{a\top}(C\gamma_5)d^b]u^c$ and $\chi_2 = \epsilon^{abc}[u^{a\top}(C)d^b]\gamma_5 u^c$, with 16, 35, 100, or 200 sweeps of gauge-invariant Gaussian smearing [16] applied at the quark source and sinks in creating the propagators. For each level of smearing, we calculate 3200 quark propagators by making use of eight shifted sources on an ensemble of 400 gauge field configurations. We perform both analyses and extract the effective energies of the states at the seven momenta described in Table I, ranging from $\boldsymbol{p}^2 = 0.166$ GeV^2 to $\boldsymbol{p}^2 = 0.996$ GeV^2.

We can gain insight into the amount of "leakage" between different parity sectors by considering the correlation matrix eigenvector elements corresponding to operators that couple primarily to states of the opposite parity. In Fig. 1 we plot the eigenvector components of the four lowest lying states isolated by the 16×16 expanded basis correlation matrix at each of the seven momenta. The coloration of the data points correspond to the operator structure associated with that component of the eigenvector ($\chi_1^+ = \Gamma_{\boldsymbol{p}}\chi_1$, $\chi_2^+ = \Gamma_{\boldsymbol{p}}\chi_2$, $\chi_1^- = \Gamma_{\boldsymbol{p}}\gamma_5\chi_1$, or $\chi_2^- = \Gamma_{\boldsymbol{p}}\gamma_5\chi_2$) and the shapes of the data points correspond to the number of sweeps of gauge-invariant Gaussian smearing applied in creating the propagators.

If we start by examining the first extracted state, shown in Fig. 1(a), we see that the eigenvectors at all momenta are dominated by the components in the left-hand plot, corresponding to the positive parity operators. In particular, at zero momentum, the contributions from the negative parity operators (in the right-hand plot) are consistent with zero. This clearly indicates that it is a positive parity state, as expected for the ground state nucleon. If we now look at the next extracted state, shown in Fig. 1(b), we see that this time

TABLE I. Momenta used in this analysis. Physical units are obtained from $\boldsymbol{p}$ (l.u.) by multiplying by $2\pi/32a$, with $a = 0.0951$ fm.

#	$\boldsymbol{p}$ (l.u.)	$\boldsymbol{p}^2$ (GeV^2)
1	(0,0,0)	0.000
2	(1,0,0)	0.166
3	(1,1,0)	0.332
4	(1,1,1)	0.498
5	(2,0,0)	0.664
6	(2,1,0)	0.830
7	(2,1,1)	0.996

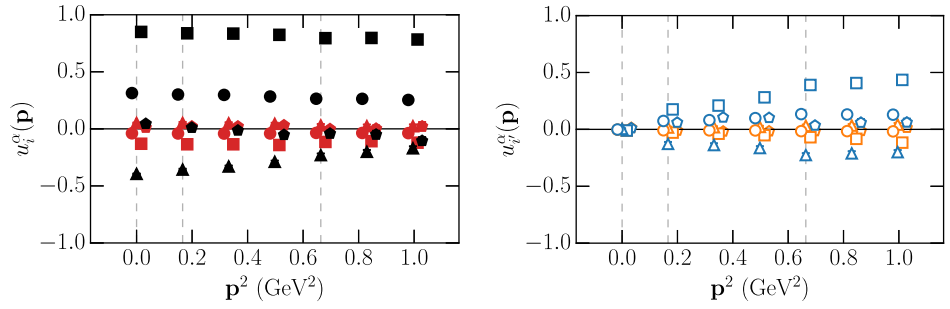

(a) The positive parity ground state nucleon.

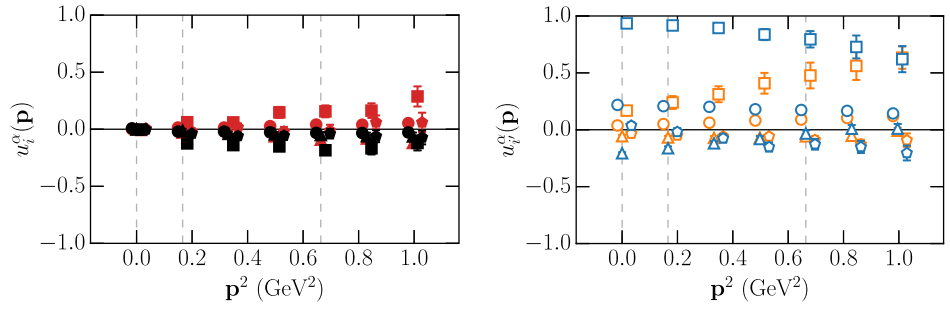

(b) The first negative parity excitation of the nucleon.

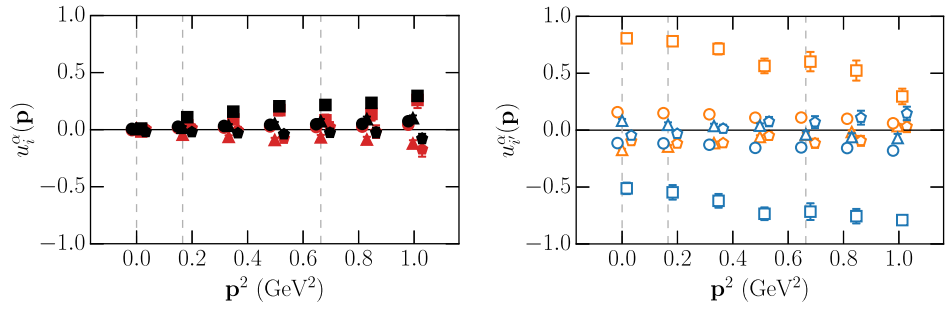

(c) The second negative parity excitation of the nucleon.

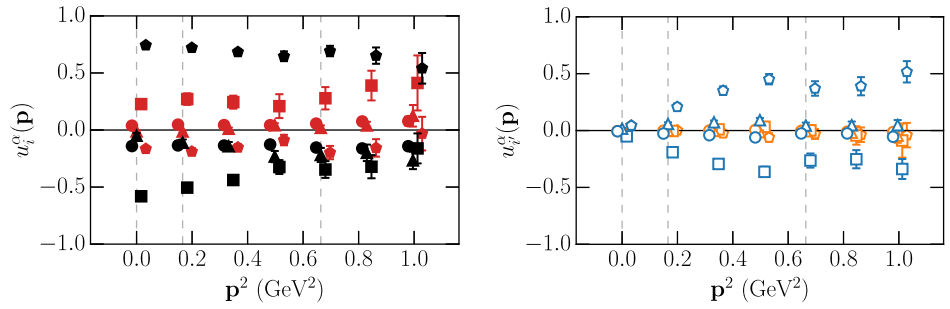

(d) The first positive parity excitation of the nucleon.

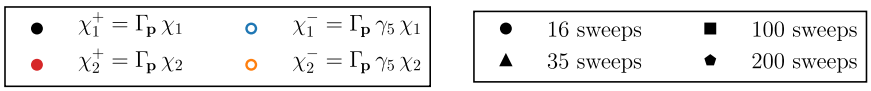

FIG. 1 (color online). Momentum-squared dependence of the PEVA eigenvectors associated with the ground state nucleon and first three excitations, showing the contribution from positive parity operators (χ_1^+, χ_2^+), negative parity operators (χ_1^-, χ_2^-), and different levels of gauge-invariant Gaussian smearing (16, 35, 100, and 200 sweeps).

the eigenvectors are dominated by the components in the right-hand plot, corresponding to the negative parity operators, and the contribution from positive parity operators at zero momentum is consistent with zero. This clearly indicates that this is a negative parity state, the first negative parity excitation of the nucleon. The next two states, shown in Figs. 1(c) and 1(d), show similarly clear parity signals, corresponding to the second negative parity and the first positive parity excitation of the nucleon respectively.

While the contributions from opposite-parity operators at zero momentum are consistent with zero, at nonzero momentum we see statistically significant contributions from operators of both parities. This is observed for all four states, even at a single lattice unit of momentum. This demonstrates that parity mixing has a significant effect on the operator structure of states at all nonzero momenta accessible on the lattice. This will have nontrivial implications for calculating three-point functions, but it is interesting to consider the simplest case of the effect on two-point functions and determinations of the effective energy.

For each state, we first fit the eigenstate-projected correlators at $\boldsymbol{p} = (0,0,0)$ with a single-state ansatz and find a fit window which produces an acceptable χ^2/degrees of freedom (DOF). We then step through the lattice momenta listed in Table I in ascending order, keeping the lower bound of the fit window fixed. The upper bound of the fit window is reduced as necessary to remove excessively noisy points. For each state at each nonzero momenta, the χ^2/DOF for a fit to our single state ansatz is calculated for the resulting fit window. High values of the χ^2/DOF indicate that the correlator suffers from contamination by multiple states. Since they produce the same correlators at zero momentum, this process results in the same fit windows for states extracted by both the 16×16 PEVA correlation matrix and the conventional 8×8 correlation matrices projected by Γ^+ and Γ^-.

Figure 2 provides a comparison of the states extracted by the conventional 8×8 correlation matrices and the states extracted by the 16×16 PEVA correlation matrix. The upper panel of Fig. 2 shows the effective energies for each state as a function of momentum. We expect the effective energy of the energy eigenstates to follow the dispersion relation $E_\alpha = \sqrt{m_\alpha^2 + \boldsymbol{p}^2}$. These are plotted on the graph as shaded bands for each state α. The lower panel of Fig. 2 shows the χ^2/DOF values for each of these fits. Contamination of our projected states shows up as a failure of the single-state ansatz as indicated by high χ^2/DOF.

We see an acceptable χ^2/DOF distribution for all fits other than those for the first negative parity excitation as extracted by the conventional 8×8 correlation matrices (open triangles). Due to the faster-decaying exponential dependence of excited state contaminations, the ground state effective energy can be cleanly extracted even when contaminated by opposite-parity states. The effective mass for the first positive parity excitation and the second

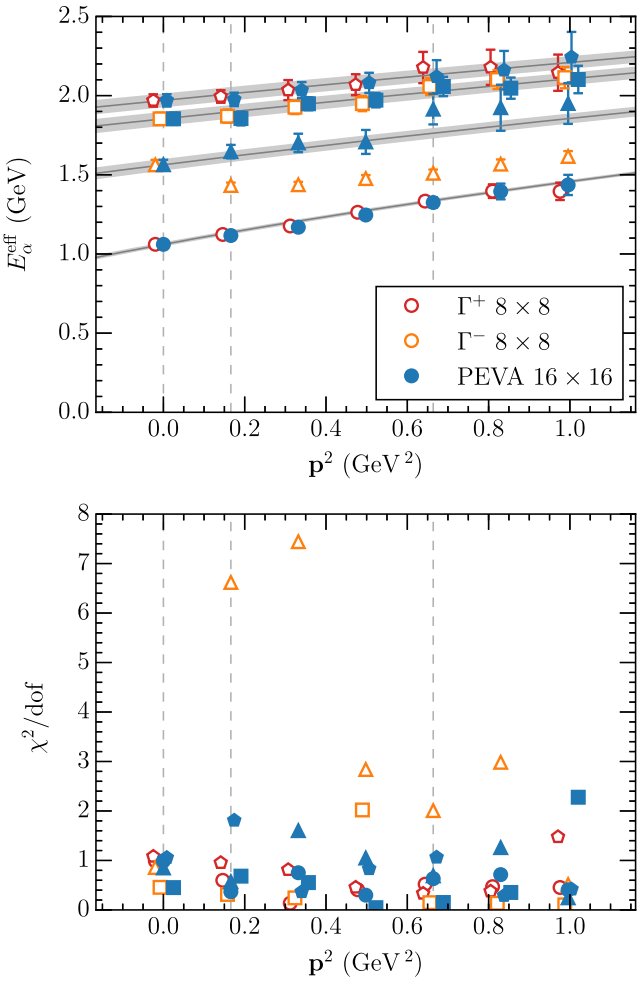

FIG. 2 (color online). Momentum-squared dependence of the effective energy fits (upper panel) and associated χ^2/DOF (lower panel) for the ground state (○), first (△) and second (□) negative parity excitations, and first positive parity excitation (⬠) of the nucleon. Results are plotted for both the full 16×16 PEVA technique (filled points) and the conventional 8×8 analyses projected by Γ^+ and Γ^- (open points). Shaded bands indicate the expected dispersion relation ($E_\alpha = \sqrt{m_\alpha^2 + \boldsymbol{p}^2}$). The ground state and the first negative parity excitation extracted by the PEVA technique are displayed at the actual momenta used, while other points are offset where necessary for clarity.

negative parity excitation do not appear to suffer from significant cross-parity contamination. However the eigenvector structure shown in Figs. 1(c) and 1(d) suggests that these states do have nontrivial opposite-parity contributions at finite momentum. A likely explanation for this is that the contaminating states are either close in energy to the eigenstate being projected, so they do not significantly change the correlator, or they have significantly higher energy, so like the ground state, the correlator is protected by Euclidean time evolution.

In the case of the first negative parity excitation, we do see significant cross-parity mixing. For the conventional

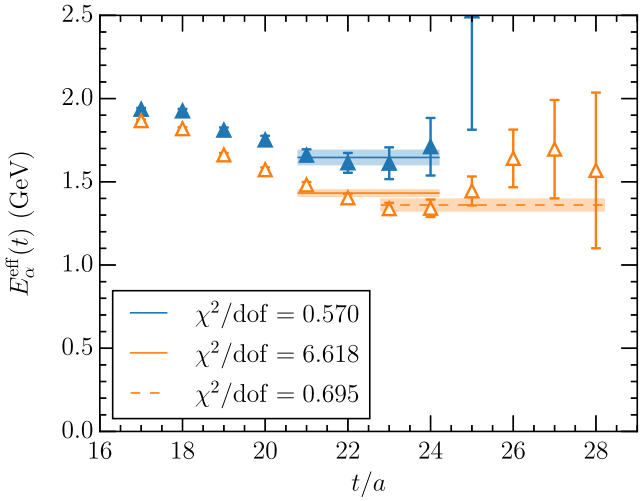

FIG. 3 (color online). Euclidean time dependence of the effective energy of the first negative parity excitation at $\boldsymbol{p} = (1,0,0)$. The effective energy of the state isolated by the conventional 8×8 correlation matrix (open symbols) has a clear nontrivial time dependence all the way up to where the signal disappears into noise, with no clear plateau, and lies significantly below the state projected by the 16×16 PEVA correlation matrix (filled symbols). The fits indicated by the solid lines are obtained using the systematic method described in Sec. IV and give the values used in Fig. 2. In the case of the conventional 8×8 correlation matrix (open symbols), this fit has an unfavorable χ^2/DOF of 6.6, indicating that multiple states are present in the correlator. A significant deviation from the systematic approach used here would allow us to move the lower bound of the fit window to a later time slice of $t/a = 24$, and take advantage of the degradation of the signal-to-noise ratio to find an acceptable χ^2/DOF. This fit, indicated by the dashed line, has a χ^2/DOF of 0.70 and a value of $1.36 \pm 0.04(\mathrm{stat}) \pm 0.14(\mathrm{syst})$, where the estimate of the systematic error is obtained by considering multiple fit windows with acceptable χ^2/DOF.

8×8 correlation matrix analysis the extracted effective energies lie between the dispersion relations for the first negative parity excitation and the ground state, which along with high χ^2/DOF values clearly indicates contamination by the (opposite-parity) ground state. By contrast the PEVA technique provides fits with an acceptable χ^2/DOF distribution, allowing us to remove these opposite-parity contaminations and cleanly isolate this first negative parity excited state, as illustrated in Fig. 3.

V. CONCLUSION

We have shown that conventional baryon spectroscopy methods applied at nonzero momentum can produce correlators that are significantly contaminated by opposite-parity states. This could in turn lead to significant errors in the determination of three-point correlation functions. We have presented the PEVA technique to address and resolve this issue. The method is equivalent to conventional parity projection methods at zero momentum, but at nonzero momentum effectively removes opposite-parity contaminations. This can have a marked effect on two-point correlation functions, such as that for the lowest lying negative parity excitation of the nucleon as shown in Sec. IV. The approach is cost effective as the basis expansion amounts to simply pre- or postmultiplying (or both) the projection matrix $\Gamma_{\boldsymbol{p}}$ by γ_5. The PEVA technique isolates nonzero momentum energy eigenstates while maintaining a signature of the state's rest-frame parity, key to understanding the content of finite momentum spectra in lattice QCD.

ACKNOWLEDGMENTS

This research was undertaken with the assistance of resources from the National Computational Infrastructure (NCI), which is supported by the Australian Government, and by resources provided by the Pawsey Supercomputing Centre with funding from the Australian Government and the Government of Western Australia. These resources were provided through the National Computational Merit Allocation Scheme and the University of Adelaide partner share. This research is supported by the Australian Research Council under ARC Discovery Projects No. DP120104627, No. DP140103067, and No. DP150103164.

APPENDIX: DIRAC STRUCTURE

To factor out the Dirac structure from Eq. (16), we substitute in the expressions from Eq. (15), and use the relation $\Gamma_{\boldsymbol{p}}(-\mathrm{i}\gamma \cdot p + m_B)\Gamma_{\boldsymbol{p}} = \Gamma_{\boldsymbol{p}}(E_B + m_B)$ to write

$$\begin{aligned}
\mathcal{G}_{ij}(\boldsymbol{p},t) &= \sum_{B^+,s} \mathrm{e}^{-E_{B^+}t} \lambda_i^{B^+} \bar{\lambda}_j^{B^+} \frac{m_{B^+}}{E_{B^+}} \Gamma_{\boldsymbol{p}} u_{B^+}(p,s) \bar{u}_{B^+}(p,s) \Gamma_{\boldsymbol{p}} + \sum_{B^-,s} \mathrm{e}^{-E_{B^-}t} \lambda_i^{B^-} \bar{\lambda}_j^{B^-} \frac{m_{B^-}}{E_{B^-}} \frac{|\boldsymbol{p}|^2}{(E_{B^-}+m_{B^-})^2} \Gamma_{\boldsymbol{p}} u_{B^-}(p,s) \bar{u}_{B^-}(p,s) \Gamma_{\boldsymbol{p}} \\
&= \sum_{B^+} \mathrm{e}^{-E_{B^+}t} \lambda_i^{B^+} \bar{\lambda}_j^{B^+} \Gamma_{\boldsymbol{p}} \frac{-\mathrm{i}\gamma \cdot p + m_{B^+}}{2E_{B^+}} \Gamma_{\boldsymbol{p}} + \sum_{B^-} \mathrm{e}^{-E_{B^-}t} \lambda_i^{B^-} \bar{\lambda}_j^{B^-} \left(\frac{E_{B^-} - m_{B^-}}{E_{B^-} + m_{B^-}} \right) \Gamma_{\boldsymbol{p}} \frac{-\mathrm{i}\gamma \cdot p + m_{B^-}}{2E_{B^-}} \Gamma_{\boldsymbol{p}} \\
&= \Gamma_{\boldsymbol{p}} \left[\sum_{B^\pm} \mathrm{e}^{-E_{B^\pm}t} \lambda_i^{B^\pm} \bar{\lambda}_j^{B^\pm} \frac{E_{B^\pm} \pm m_{B^\pm}}{2E_{B^\pm}} \right], \qquad \text{(A1a)}
\end{aligned}$$

$$\mathcal{G}_{ij'}(\boldsymbol{p},t) = \mathcal{G}_{i'j}(\boldsymbol{p},t)$$
$$= \sum_{B^\pm} \mathrm{e}^{-E_{B^\pm}t} \lambda_i^{B^\pm} \bar{\lambda}_j^{B^\pm} \frac{|\boldsymbol{p}|}{E_{B^\pm}+m_{B^\pm}} \Gamma_{\boldsymbol{p}} \frac{-\mathrm{i}\gamma\cdot p + m_{B^\pm}}{2E_{B^\pm}} \Gamma_{\boldsymbol{p}}$$
$$= \Gamma_{\boldsymbol{p}} \left[\sum_{B^\pm} \mathrm{e}^{-E_{B^\pm}t} \lambda_i^{B^\pm} \bar{\lambda}_j^{B^\pm} \frac{|\boldsymbol{p}|}{2E_{B^\pm}} \right], \tag{A1b}$$

$$\mathcal{G}_{i'j'}(\boldsymbol{p},t) = \sum_{B^+,s} \mathrm{e}^{-E_{B^+}t} \lambda_i^{B^+} \bar{\lambda}_j^{B^+} \left(\frac{E_{B^+}-m_{B^+}}{E_{B^+}+m_{B^+}} \right) \Gamma_{\boldsymbol{p}} \frac{-\mathrm{i}\gamma\cdot p + m_{B^+}}{2E_{B^+}} \Gamma_{\boldsymbol{p}} + \sum_{B^-,s} \mathrm{e}^{-E_{B^-}t} \lambda_i^{B^-} \bar{\lambda}_j^{B^-} \Gamma_{\boldsymbol{p}} \frac{-\mathrm{i}\gamma\cdot p + m_{B^-}}{2E_{B^-}} \Gamma_{\boldsymbol{p}}$$
$$= \Gamma_{\boldsymbol{p}} \left[\sum_{B^\pm} \mathrm{e}^{-E_{B^\pm}t} \lambda_i^{B^\pm} \bar{\lambda}_j^{B^\pm} \frac{E_{B^\pm} \mp m_{B^\pm}}{2E_{B^\pm}} \right]. \tag{A1c}$$

Now, if we right multiply the traced correlation matrix $G(\boldsymbol{p},t)$ by the column vector

$$\boldsymbol{u}^{\alpha^+}(\boldsymbol{p}) \equiv (u_1^{\alpha^+}(\boldsymbol{p}), \ldots, u_n^{\alpha^+}(\boldsymbol{p}), u_{1'}^{\alpha^+}(\boldsymbol{p}), \ldots, u_{n'}^{\alpha^+}(\boldsymbol{p}))^\top$$

corresponding to the positive parity state B^{α^+}, then the components of the resulting vector are given by

$$(G(\boldsymbol{p},t)\boldsymbol{u}^{\alpha^+}(\boldsymbol{p}))_i = G_{ij}(\boldsymbol{p},t) u_j^{\alpha^+}(\boldsymbol{p}) + G_{ij'}(\boldsymbol{p},t) u_{j'}^{\alpha^+}(\boldsymbol{p})$$
$$= \mathrm{tr}\left(\sum_{B^\beta,s} \mathrm{e}^{-E_\beta t} \langle \Omega | \chi_{\boldsymbol{p}}^i | B^\beta; p; s \rangle \langle B^\beta; p; s | \bar{\phi}_{\boldsymbol{p}}^{\alpha^+} | \Omega \rangle \right)$$
$$= \mathrm{tr}\left(\sum_{B^\beta,s} \mathrm{e}^{-E_{\alpha^+}t} \delta^{\alpha^+\beta} \lambda_i^{\alpha^+} \bar{z}^{\alpha^+} \frac{m_{\alpha^+}}{E_{\alpha^+}} \Gamma_{\boldsymbol{p}} u_{\alpha^+}(p,s) \bar{u}_{\alpha^+}(p,s) \Gamma_{\boldsymbol{p}} \right)$$
$$= \mathrm{tr}\left(\mathrm{e}^{-E_{\alpha^+}t} \lambda_i^{\alpha^+} \bar{z}^{\alpha^+} \Gamma_{\boldsymbol{p}} \frac{-\mathrm{i}\gamma\cdot p + m_{\alpha^+}}{2E_{\alpha^+}} \Gamma_{\boldsymbol{p}} \right)$$
$$= \mathrm{e}^{-E_{\alpha^+}t} \lambda_i^{\alpha^+} \bar{z}^{\alpha^+} \frac{E_{\alpha^+}+m_{\alpha^+}}{2E_{\alpha^+}}, \tag{A2a}$$

$$(G(\boldsymbol{p},t)\boldsymbol{u}^{\alpha^+}(\boldsymbol{p}))_{i'} = G_{i'j}(\boldsymbol{p},t) u_j^{\alpha^+}(\boldsymbol{p}) + G_{i'j'}(\boldsymbol{p},t) u_{j'}^{\alpha^+}(\boldsymbol{p})$$
$$= \mathrm{tr}\left(\sum_{B^\beta,s} \mathrm{e}^{-E_{\alpha^+}t} \delta^{\alpha^+\beta} \lambda_i^{\alpha^+} \bar{z}^{\alpha^+} \frac{|\boldsymbol{p}|}{E_{\alpha^+}+m_{\alpha^+}} \frac{m_{\alpha^+}}{E_{\alpha^+}} \Gamma_{\boldsymbol{p}} u_{\alpha^+}(p,s) \bar{u}_{\alpha^+}(p,s) \Gamma_{\boldsymbol{p}} \right)$$
$$= \mathrm{e}^{-E_{\alpha^+}t} \lambda_i^{\alpha^+} \bar{z}^{\alpha^+} \frac{|\boldsymbol{p}|}{2E_{\alpha^+}}. \tag{A2b}$$

Here we have the overlap of the perfect operator $\bar{\phi}_{\boldsymbol{p}}^{\alpha^+}$ with some state B^β, as given in Eq. (13), which introduces the term $\delta^{\alpha^+\beta}\bar{z}^{\alpha^+}$, eliminating the sum over states and leaving us with a single energy eigenstate α^+.

[1] S. Aoki *et al.* (PACS-CS Collaboration), 2 + 1 flavor lattice QCD toward the physical point, Phys. Rev. D **79**, 034503 (2009).

[2] A. Bazavov *et al.* (MILC Collaboration), Nonperturbative QCD simulations with 2 + 1 flavors of improved staggered quarks, Rev. Mod. Phys. **82**, 1349 (2010).

[3] S. Durr *et al.*, Ab initio determination of light hadron masses, Science **322**, 1224 (2008).

[4] Z. Fodor and C. Hoelbling, Light hadron masses from lattice QCD, Rev. Mod. Phys. **84**, 449 (2012).

[5] A. L. Kiratidis, W. Kamleh, D. B. Leinweber, and B. J. Owen, Lattice baryon spectroscopy with multiparticle interpolators, Phys. Rev. D **91**, 094509 (2015).

[6] M. S. Mahbub, W. Kamleh, D. B. Leinweber, P. J. Moran, and A. G. Williams, Structure and flow of the nucleon eigenstates in lattice QCD, Phys. Rev. D **87**, 094506 (2013).
[7] M. S. Mahbub, W. Kamleh, D. B. Leinweber, P. J. Moran, and A. G. Williams (CSSM Lattice Collaboration), Roper resonance in $2+1$ flavor QCD, Phys. Lett. B **707**, 389 (2012).
[8] R. G. Edwards, N. Mathur, D. G. Richards, and S. J. Wallace (Hadron Spectrum Collaboration), Flavor structure of the excited baryon spectra from lattice QCD, Phys. Rev. D **87**, 054506 (2013).
[9] R. G. Edwards, J. J. Dudek, D. G. Richards, and S. J. Wallace, Excited state baryon spectroscopy from lattice QCD, Phys. Rev. D **84**, 074508 (2011).
[10] V. Verduci and C. B. Lang, Baryon resonances coupled to Pion-Nucleon states in lattice QCD, *Proc. Sci.*, LATTICE2014 (2014) 121 [arXiv:1412.0701].
[11] C. Lang and V. Verduci, Scattering in the πN negative parity channel in lattice QCD, Phys. Rev. D **87**, 054502 (2013).
[12] C. Alexandrou, T. Leontiou, C. N. Papanicolas, and E. Stiliaris, Novel analysis method for excited states in lattice QCD: The nucleon case, Phys. Rev. D **91**, 014506 (2015).
[13] M. G. Beckett, B. Joo, C. M. Maynard, D. Pleiter, O. Tatebe, and T. Yoshie, Building the international lattice data grid, Comput. Phys. Commun. **182**, 1208 (2011).
[14] F. X. Lee and D. B. Leinweber, Negative-parity baryon spectroscopy, Nucl. Phys. B, Proc. Suppl. **73**, 258 (1999).
[15] R. W. Schiel, Expanding the interpolator basis in the variational method to explicitly account for backward running states, Phys. Rev. D **92**, 034512 (2015).
[16] S. Gusken, A study of smearing techniques for hadron correlation functions, Nucl. Phys. B, Proc. Suppl. **17**, 361 (1990).